

Signatures of the Higgs mode in transport through a normal-metal–superconductor junction

Gaomin Tang,¹ Wolfgang Belzig,² Ulrich Zülicke,³ and Christoph Bruder¹

¹*Department of Physics, University of Basel, Klingelbergstrasse 82, CH-4056 Basel, Switzerland*

²*Fachbereich Physik, Universität Konstanz, D-78457 Konstanz, Germany*

³*School of Chemical and Physical Sciences and MacDiarmid Institute for Advanced Materials and Nanotechnology, Victoria University of Wellington, P.O. Box 600, Wellington 6140, New Zealand*

A superconductor subject to electromagnetic irradiation in the terahertz range can show amplitude oscillations of its order parameter. However, coupling this so-called Higgs mode to the charge current is notoriously difficult. We propose to achieve such a coupling in a particle-hole-asymmetric configuration using a DC-voltage-biased normal-metal–superconductor tunnel junction. Using the quasiclassical Green’s function formalism, we demonstrate three characteristic signatures of the Higgs mode: (i) The AC charge current exhibits a pronounced resonant behavior and is maximal when the radiation frequency coincides with the order parameter. (ii) The AC charge current amplitude exhibits a characteristic nonmonotonic behavior with increasing voltage bias. (iii) At resonance for large voltage bias, the AC current vanishes inversely proportional to the bias. These signatures provide an electric detection scheme for the Higgs mode.

Introduction.— Manipulating the superconducting (SC) state using tailored light pulses is currently receiving a great deal of attention. Various fascinating phenomena have been reported, including superconductivity enhancement [1–6], light-induced superconductivity [7–10], the presence of chiral Majorana modes in chiral superconductors [11], and the emergence of the Higgs mode [12–38].

The Higgs mode is a gapped collective excitation consisting of the oscillation of the order parameter amplitude in a system with spontaneous symmetry breaking [12–15]. In a superconductor where the $U(1)$ symmetry is spontaneously broken, the order parameter amplitude can oscillate when the system is coupled to external gauge fields. The presence of a Higgs mode in superconductors with charge density waves was first observed using the Raman-scattering technique [16–18] and later theoretically interpreted [19, 20]. However, the excitation and detection of the Higgs mode in superconductors without charge density waves became experimentally possible only in the last decade due to the experimental advance of ultrafast low-energy terahertz (THz) spectroscopy. Clear non-linear optical signatures indicating the presence of a Higgs mode have been observed using the pump-probe technique in both s -wave [21–24, 26] and d -wave [27] superconductors. Since the Higgs mode is a scalar excitation, it is expected to couple to the external electromagnetic field in a nonlinear way. A linear coupling enabled by the presence of a supercurrent was theoretically proposed [30] and experimentally verified [31]. Very recently, it was theoretically predicted that a Higgs mode can be observed through its effect in the time-dependent spin current in a ferromagnet-superconductor junction [28].

In this work, we consider a junction between a normal metal and an s -wave superconductor [see Fig. 1(a)]. THz electromagnetic irradiation can excite a Higgs mode on the SC part of the junction. To couple the Higgs mode to the charge current, particle-hole symmetry has to be broken. Inducing a finite spin splitting in the superconductor is one way to achieve this [28]. As a potentially simpler alternative, we propose to apply a DC voltage bias to a normal-metal–superconductor (NS) junction. We demonstrate that the Higgs mode will manifest

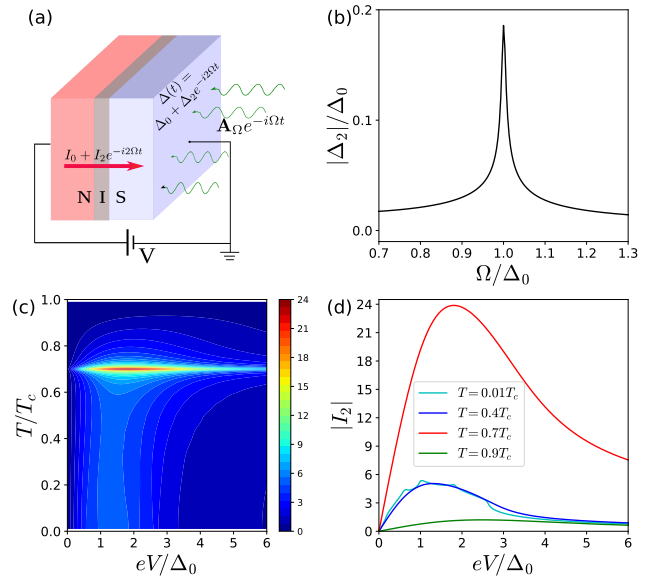


FIG. 1. (a) DC-voltage-biased normal-metal–superconductor (NS) junction with a thin insulator (I) acting as a tunnel barrier. The superconductor is subject to electromagnetic irradiation described by a time-dependent vector potential $\mathbf{A}_\Omega e^{-i\Omega t}$, which generates a Higgs mode inside the superconductor. (b) $|\Delta_2|/\Delta_0$ as a function of Ω/Δ_0 . The parameters are chosen as $T = 0.05T_c$, $\gamma = 0.01\Delta_0|_{T=0}$, and $W_A = 0.01\Delta_0|_{T=0}$. (c) AC charge current $|I_2|$ plotted against temperature T and bias voltage eV scaled by the static SC gap amplitude at temperature T . The charge currents are in units of $G_t W_A/e$. The electromagnetic frequency is set to be $\Omega = \Delta_0|_{T=0.7T_c}$. (d) Line cuts of (c) at different temperatures.

itself in intriguing properties of the AC charge current through the junction [see Fig. 1(c)].

Higgs mode in the superconductor.— We consider a superconductor subject to monochromatic electromagnetic irradiation with the time-dependent vector potential $\mathbf{A}(t) = \mathbf{A}_\Omega e^{-i\Omega t}$ in the Coulomb gauge. Due to the nonlinear coupling between the electromagnetic field and the Higgs mode, there will be a second-harmonic correction to the static SC

gap Δ_0 . Thus, the time-dependent order parameter can be expressed as

$$\langle \Delta(t) \rangle = \Delta_0 + \Delta_2 e^{-i2\Omega t}. \quad (1)$$

If the irradiation frequency is close to Ω_0 , superconductivity can possibly be enhanced [3, 4], and a small correction to the static order parameter can be incorporated in Δ_0 .

We employ the quasiclassical Green's function technique to study the dynamics of the superconductor and the transport properties of the NS junction. The quasiclassical Green's function $g_s(t, t')$ for a dirty superconductor with the diffusion constant D fulfills the time-dependent Usadel equation [39, 40]

$$i \{ \tau_3 \partial_t, g_s \} + [\mathbf{A}, g_s] - iD \nabla (g_s \circ \nabla g_s) = 0, \quad (2)$$

where the Green's function is written in Keldysh space and has the structure

$$g_s = \begin{pmatrix} \hat{g}_s^r & \hat{g}_s^k \\ 0 & \hat{g}_s^a \end{pmatrix}. \quad (3)$$

The order parameter has the form $\Delta = i\tau_2 \Delta$. The matrices τ_α with $\alpha = 1, 2, 3$ are diagonal matrices with entries $\hat{\tau}_\alpha$, that is $\tau_\alpha = \text{diag}[\hat{\tau}_\alpha, \hat{\tau}_\alpha]$, where $\hat{\tau}_\alpha$ are the Pauli matrices in Nambu space. In Eq. (2), the anti-commutator is defined as $\{ \tau_3 \partial_t, g_s \} = \tau_3 \partial_t g_s(t, t') + \partial_{t'} g_s(t, t') \tau_3$, and $\nabla \cdot = \partial_{\mathbf{r}} \cdot - ie[\tau_3 \mathbf{A}(t), \cdot]$. The convolution operation between two objects f and g is defined as $(f \circ g)(t, t') = \int dt_1 f(t, t_1) g(t_1, t')$. The Green's function obeys the normalization condition $g_s \circ g_s = 1$.

Since the Higgs mode couples to the electromagnetic field nonlinearly, to leading order there is a second-harmonic correction g_2 to the stationary Green's function g_0 ,

$$g_s(t, t') = g_0(t - t') + g_2(t, t'). \quad (4)$$

The Fourier transforms of g_0 and g_2 are, respectively, defined as

$$\begin{aligned} g_0(t - t') &= \int \frac{d\epsilon}{2\pi} e^{-i\epsilon(t-t')} g_0(\epsilon), \\ g_2(t, t') &= \int \frac{d\epsilon}{2\pi} e^{-i\epsilon_+ t + i\epsilon_- t'} g_2(\epsilon_+, \epsilon_-), \end{aligned} \quad (5)$$

with $\epsilon_\pm = \epsilon \pm \Omega$. The normalization condition leads to $g_2(\epsilon_+, \epsilon_-) g_0(\epsilon_-) + g_0(\epsilon_+) g_2(\epsilon_+, \epsilon_-) = 0$.

For the stationary quasiclassical Green's functions, we have [40]

$$\hat{g}_0^{r(a)}(\epsilon) = g_0^{r(a)}(\epsilon) \hat{\tau}_3 + i \hat{\tau}_2 f_0^{r(a)}(\epsilon), \quad (6)$$

$$\hat{g}_0^k(\epsilon) = [\hat{\gamma}_0^r(\epsilon) - \hat{g}_0^a(\epsilon)] \tanh(\beta\epsilon/2), \quad (7)$$

where $\beta = 1/(k_B T)$, and

$$g_0^{r(a)} = f_0^{r(a)} \epsilon / \Delta_0 = \epsilon / s_0^{r(a)}, \quad (8)$$

with $s_0^{r(a)} = i\sqrt{\frac{\Delta_0^2}{2} - (\epsilon \pm i\gamma)^2}$. Here, γ is the phenomenological Dynes broadening parameter. Inserting Eqs. (1) and

(4) into the Usadel equation (2) leads to the retarded and advanced components of the nonstationary term [28],

$$\hat{g}_2^{r(a)}(\epsilon_+, \epsilon_-) = \hat{\gamma}_V^{r(a)}(\epsilon_+, \epsilon_-) + \hat{\gamma}_H^{r(a)}(\epsilon_+, \epsilon_-). \quad (9)$$

The first term $\hat{\gamma}_V$ is due to the direct second-order coupling to the vector potential and reads

$$\hat{\gamma}_V^{r(a)}(\epsilon_+, \epsilon_-) = iW_A \left[\frac{\hat{g}_0(\epsilon) - \hat{g}_0(\epsilon_+) \hat{g}_0(\epsilon) \hat{g}_0(\epsilon_-)}{s_+ + s_-} \right]^{r(a)}, \quad (10)$$

with $W_A = De^2 |\mathbf{A}_\Omega|^2$ and $\hat{g}_0 = \hat{\tau}_3 \hat{g}_0 \hat{\tau}_3$. The second term $\hat{\gamma}_H$ describes the effect of the Higgs mode,

$$\hat{\gamma}_H^{r(a)}(\epsilon_+, \epsilon_-) = i \left[\frac{\hat{\tau}_2 - \hat{g}_0(\epsilon_+) \hat{\tau}_2 \hat{g}_0(\epsilon_-)}{s_+ + s_-} \right]^{r(a)}. \quad (11)$$

Both here and in (10), we have used the notation $s_\pm^{r(a)} = i\sqrt{\frac{\Delta_0^2}{2} - (\epsilon_\pm \pm i\gamma)^2}$ and $s_\pm^{r(a)} = i\sqrt{\frac{\Delta_0^2}{2} - (\epsilon_\pm \pm i\gamma)^2}$.

An expression for the oscillating part Δ_2 of the SC gap can be obtained from the gap equation $\langle \Delta(t) \rangle = -i\lambda \text{Tr}[\hat{\tau}_2 \hat{g}_s^k(t)]$, where λ is the pairing interaction. The details of the derivation can be found in the Supplemental Material [41]. The static order parameter Δ_0 at temperature T (denoted by $\Delta_0(T)$) can be well fitted by the interpolation formula

$$\Delta_0(T) = \Delta_0|_{T=0} \tanh(1.74\sqrt{T_c/T - 1}), \quad (12)$$

where T_c is the critical temperature. To simplify the notation, we will omit the variable T in $\Delta_0(T)$ at nonzero temperature.

The Dynes broadening parameter and irradiation intensity are fixed as $\gamma = 0.01 \Delta_0|_{T=0}$ and $W_A = 0.01 \Delta_0|_{T=0}$ in this work. In Fig. 1(b), we plot the dependence of Δ_2 on the irradiation frequency Ω at temperature $T = 0.05T_c$. A cusp appears at $\Omega = \Omega_0$ (resonant condition) where the oscillation amplitude of the order parameter $|\Delta_2|$ is maximal. The resonant behavior is a signature of the Higgs mode and can be identified in nonlinear optical response using the pump-probe technique [21–24, 26].

Normal-metal–superconductor junction.—In the following, we study the transport properties of a DC-voltage-biased NS junction, in which the SC side is subject to electromagnetic irradiation described by a vector potential $\mathbf{A}(t) = \mathbf{A}_\Omega e^{-i\Omega t}$ [see Fig. 1(a)]. The THz electromagnetic field is assumed to exist only on the SC side to avoid possible photon-assisted tunneling processes, and its wave vector is parallel to the transport direction of the junction. The thickness of the superconductor is assumed to be smaller than or comparable to the SC coherence length, so that the order parameter can be treated as homogeneous. For simplicity, we consider a tunnel junction, which is characterized by its conductance G_t . The retarded, advanced and Keldysh components of the Green's function for the normal metal are expressed as

$$\hat{g}_n^r = -\hat{g}_n^a = \hat{\tau}_3, \quad (13)$$

and

$$\hat{g}_n^k(\epsilon) = 2 \text{diag} \left[\tanh\left(\frac{\epsilon - eV}{2k_B T}\right), -\tanh\left(\frac{\epsilon + eV}{2k_B T}\right) \right], \quad (14)$$

where V is the external voltage bias.

Since the leading perturbation due to the Higgs mode is a second harmonic in ϕ , the electric current $I(t)$ can be decomposed in a DC component I_0 and an AC component I_2 with $I(t) = I_0 + I_2 e^{-i2\Omega t}$. For a tunnel junction, the AC component of the particle current to the first order in the tunnel conductance is

$$I_2 = \frac{G_t}{8e} \int d\epsilon \text{Tr}(\mathcal{A}_3 \hat{X}), \quad (15)$$

with

$$\hat{X} = \mathcal{G}_n^k(\epsilon_+) \mathcal{G}_2^a(\epsilon_+, \epsilon_-) - \mathcal{G}_2^r(\epsilon_+, \epsilon_-) \mathcal{G}_n^k(\epsilon_-). \quad (16)$$

Equation (15) implies that $I_2|_{eV=0} = 0$, since the situation is particle-hole symmetric in the absence of a DC voltage bias. A finite voltage bias can break the symmetry so that the Higgs mode can couple to the charge current. This is in contrast to Ref. [28], where particle-hole asymmetry is due to the exchange field in the superconductor induced by an external magnetic field. A detailed derivation of I_2 using circuit theory [42–44] can be found in the Supplemental Material [41].

Numerical results.— The gap oscillation amplitude Δ_2 is a complex number. This also applies to the AC charge current I_2 , and we focus on discussing the AC charge current magnitude $|I_2|$. Figures 2(a), (b) and (c) show the dependence of $|I_2|$ on the voltage bias eV and the electromagnetic frequency Ω , where panels (b) and (c) are line cuts of panel (a) for different values of Ω and eV , respectively. To illustrate the influence of the Higgs mode on transport, we artificially set $\Delta_2 = 0$ in g_2 , that is, $\mathcal{G}_2 = \mathcal{G}_V$ from Eq. (9), and calculate the corresponding AC current amplitude $|I_2^{\Delta_2=0}|$ for comparison [see Figs. 2(d), (e) and (f)]. The charge currents are shown in units of $G_t W_A/e$.

As can be seen from Fig. 2, the AC charge current amplitude $|I_2|$ at a fixed voltage bias shows a pronounced resonant behavior as a function of frequency at $\Omega = \Omega_0$, which is not present for $|I_2^{\Delta_2=0}|$. This can be easily observed by comparing Fig. 2(c) and (f) at $eV = \Omega_0$. Also, $|I_2|$ is much larger than $|I_2^{\Delta_2=0}|$ at resonance, since the SC gap oscillation amplitude $|\Delta_2|$ achieves its maximum and is much larger than W_A as can be seen from Fig. 1(b). Thus, the Higgs mode dominates the AC charge current at resonance. In Fig. S1 in the Supplemental Material [41], we compare the contributions from \mathcal{G}_V and \mathcal{G}_H in the AC charge current amplitude and find that the contribution from \mathcal{G}_V can be even larger than that from \mathcal{G}_H away from resonance. The resonant behavior of $|I_2|$ can serve as a signature of the presence of the Higgs mode in the superconductor. A similar observation has been recently reported for spin currents driven by the Higgs mode [28].

Figure 2(b) shows that $|I_2|$ exhibits an interesting non-monotonic behavior: it increases with increasing voltage bias up to around $eV = \Omega_0$, then starts to decrease. At resonance $\Omega = \Omega_0$, the AC charge current shows a peak around $eV = \Omega_0$. This is explained as follows. The Higgs mode can be interpreted as coherent depairing and pairing of Cooper

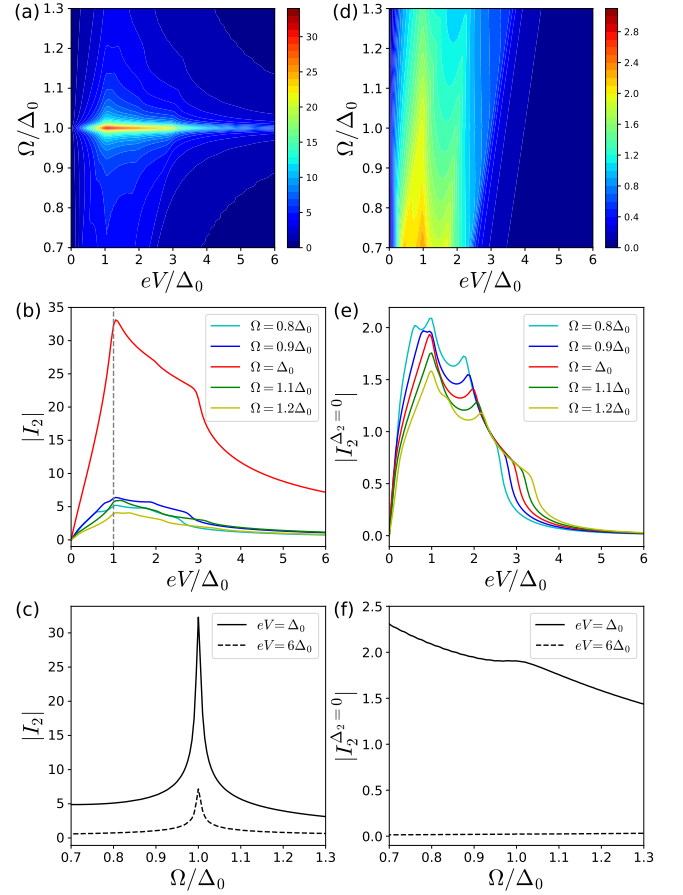


FIG. 2. (a) AC charge current $|I_2|$ plotted against voltage bias eV and irradiation frequency Ω . Panels (b) and (c) are line cuts of (a) at different Ω and eV , respectively. (d) AC charge current $|I_2^{\Delta_2=0}|$ in the absence of the Higgs mode, i.e. by artificially setting $\Delta_2 = 0$. Panels (e) and (f) are line cuts of (d) at different Ω and eV , respectively. The charge currents are in units of $G_t W_A/e$. The temperature is $T = 0.05T_c$, the other parameters are the same as in Fig. 1(b).

pairs. The characteristic frequency of the Higgs mode is $2\Omega_0$, thus the split quasiparticles (or depaired Cooper pairs) will appear around the SC band edge. Since it is the split quasiparticles that contribute to the AC charge current at resonance, the AC charge current reaches a maximum if the DC voltage bias aligns with the SC band edge at low temperatures. There is also a kink at $eV = 3\Omega_0$ that can be interpreted as a side band due to the Higgs mode that modulates the quasiparticle density.

Away from resonance, we can observe some other special points in Fig. 2(b). These points are due to the excitation from the electromagnetic irradiation with maxima at $eV = \Omega_0$, $\Omega_0 + 2\Omega_0$, $\Omega_0 + 4\Omega_0$ and a kink at $\Omega_0 + 2\Omega_0$ as can be observed from Fig. 2(e). At higher temperatures, the non-monotonic behavior of $|I_2|$ still survives, while the maximum point shifts to higher voltages with $eV > \Omega_0$ due to thermal excitations (see Fig. S2 in the Supplemental Material [41] for $T = 0.7T_c$).

Under a large bias, the AC charge current I_2 shows char-

characteristic features: even at $eV = 6\phi_0$, a resonant behavior as a function of ω can be observed in Fig. 2(c). In contrast, if the Higgs mode is not taken into account, the AC charge current $I_2^{\Delta_2=0}$ vanishes at large voltage bias even for $\omega = \phi_0$ as shown in Fig. 2(e). At resonance and with $eV \gg \phi_0$, an analytical estimate given in the Supplemental Material [41] shows that the AC current is inversely proportional to the voltage bias, i.e., $I_2 \propto \phi_0/(eV)$. Thus a finite AC charge current can persist up to relatively large voltage biases. This characteristic behavior of the AC charge current at large bias near resonance can serve as an indicator for the presence of the Higgs mode in the superconductor.

Apart from the possibility to tune the irradiation frequency continuously in experiment [45, 46], one can alternatively tune the Higgs mode to be at or away from the resonant condition by changing the system temperature [22]. In Fig. 1(c), we show the AC charge current magnitude as a function of voltage bias and temperature. The electromagnetic frequency is fixed at $\omega = \phi_0|_{T=0.7T_c} \approx 0.8\phi_0|_{T=0}$, which means that the resonance is achieved by tuning the temperature to be at $T = 0.7T_c$. This leads to a prominent resonant behavior as shown in Fig. 1(c).

Figure 1(d) also shows that $|I_2|$ exhibits a nonmonotonic behavior as a function of voltage bias. At a low temperature with $T = 0.01T_c$, $|I_2|$ reaches its maximum around $eV = \phi_0$. It also has maxima at both $0.6\phi_0 (\approx -\phi_0 + 2\phi_0)$ and $1.8\phi_0 (\approx \phi_0 + 2\phi_0)$ and a kink at $2.6\phi_0 (\approx \phi_0 + 2\phi_0)$ due to photon-assisted transport processes. Due to thermal excitations, the voltage bias at which I_2 reaches its maximum increases with increasing temperature. Once the temperature reaches the SC critical temperature, both the static SC gap amplitude and its oscillation vanish, and so does the AC charge current. Similarly to Fig. 2(b), we observe a slow decay $\propto \phi_0/(eV)$ of the AC charge current at large bias near resonance.

Since ϕ_2 is proportional to W_A [41], the next-order correction to the time-dependent order parameter $\langle \phi(t) \rangle$ in Eq. (1) is proportional to W_A^2 . Higher-order corrections to $\langle \phi(t) \rangle$ can be ignored if $W_A/\phi_0 \ll 1$ is satisfied. Given the smallness of $W_A/(\phi_0|_{T=0})$, which is 0.01 in this work, the condition $W_A/\phi_0 \ll 1$ can be satisfied if the temperature is not too close to T_c .

The AC current I_2 is given in units of $G_t W_A/e$ where G_t is the tunnel conductance of the junction and the value chosen for the coupling parameter W_A is $W_A = 0.01\phi_0|_{T=0}$. For example, for the superconductor NbN, $\phi_0|_{T=0} \approx 2.6\text{meV}$ [31], so that the values of I_2 shown in the figures are approximately in units of $0.026\text{mV} \cdot G_t$.

Discussion.— The physical picture that emerges is as follows: the pairing/depairing processes associated with the order-parameter oscillation (Higgs mode) will create particles and holes each of which contribute to the AC tunnel current. At zero voltage bias, their respective contributions cancel. A finite voltage bias leads to particle-hole asymmetry that results in a finite AC current that exhibits signatures of the Higgs mode. On the one hand, this AC charge current may be measured directly. Alternatively, the NS junction can be ex-

perimentally manufactured as an antenna, where the electromagnetic irradiation magnitude and frequency due to the AC charge current can be detected. Even though a tunnel junction is studied here, we expect all of the discussed features to be present for a highly transparent junction as well. Note that it is well established that nonequilibrium achieved by voltage biasing can affect the AC response of a superconductor (see, e.g., [47]). However, our work considers the inverse situation that the AC response of a superconductor (the Higgs mode) can affect the transport properties of a voltage-biased junction.

The order-parameter oscillation will slowly decay in a power-law way if the electromagnetic irradiation is switched off, and the same applies to the AC charge current. Here, we only treat the steady-state situation with a constant electromagnetic irradiation.

At low temperatures $T \ll \phi_0$, the conductance of the NS-junction that we consider is exponentially suppressed. Thus, for the results presented in Fig. 2, where the temperature is chosen as $T = 0.05T_c$, we do not expect Joule heating to be a severe problem, and the predicted effects will be unchanged. For the results presented in Fig. 1(c) and (d), if Joule heating exists, the resonant behavior will occur at a lower temperature. However, we expect all the qualitative features to remain.

In the work presented above, the wave vector of the electromagnetic field is assumed to be parallel to the transport direction of the junction. If the wave vector has a finite orthogonal component, the supercurrent, which can be induced by the Andreev reflection processes, will mediate a linear coupling between the Higgs mode and the electromagnetic field [30–33]. In this case, the time-dependent order parameter can be written as $\langle \phi(t) \rangle = \phi_0 + \phi_1 e^{-i\Omega t} + \phi_2 e^{-i2\Omega t}$ with an additional term of ϕ_1 compared to Eq. (1). ϕ_1 and ϕ_2 exhibit resonances at $\omega = 2\phi_0$ and $\omega = \phi_0$, respectively. AC charge transport in an NS junction in the presence of a linear coupling between the Higgs mode and the electromagnetic irradiation will be investigated in the future. The generalization to an NS junction with unconventional superconductors [27, 37, 38] may also be interesting.

Conclusion.— We have studied the AC transport properties of a DC-voltage-biased NS tunnel junction taking into account the Higgs mode in the superconductor. The pronounced resonant behavior, the characteristic nonmonotonic behavior of the AC charge current with increasing bias and its slow decay inversely proportional to the bias can serve as signatures of the presence of the Higgs mode.

Our results could be applied to design more complex superconducting devices featuring the Higgs dynamics in coupled junctions of superconducting islands. Furthermore, it will be interesting to combine Josephson effects with the Higgs mode.

Acknowledgments.— G.T. and C.B. acknowledge financial support from the Swiss National Science Foundation (SNSF) and the NCCR Quantum Science and Technology.

- [1] A. F. G. Wyatt, V. M. Dmitriev, W. S. Moore, and F. W. Sheard, Microwave-enhanced critical supercurrents in constricted tin films, *Phys. Rev. Lett.* **16**, 1166 (1966).
- [2] A. H. Dayem and J. J. Wiegand, Behavior of thin-film superconducting bridges in a microwave field, *Phys. Rev.* **155**, 419 (1967).
- [3] J.-J. Chang and D. J. Scalapino, Gap enhancement in superconducting thin films due to microwave irradiation, *J. Low Temp. Phys.* **29**, 477 (1977).
- [4] K. S. Tikhonov, M. A. Skvortsov, and T. M. Klapwijk, Superconductivity in the presence of microwaves: Full phase diagram, *Phys. Rev. B* **97**, 184516 (2018).
- [5] J. B. Curtis, Z. M. Raines, A. A. Allocca, M. Hafezi, and V. M. Galitski, Cavity quantum Eliashberg enhancement of superconductivity, *Phys. Rev. Lett.* **122**, 167002 (2019).
- [6] H. Dehghani, Z. M. Raines, V. M. Galitski, and M. Hafezi, Optical enhancement of superconductivity via targeted destruction of charge density waves, *Phys. Rev. B* **101**, 224506 (2020).
- [7] D. Fausti, R. I. Tobey, N. Dean, S. Kaiser, A. Dienst, M. C. Hoffmann, S. Pyon, T. Takayama, H. Takagi, and A. Cavalleri, Light-induced superconductivity in a stripe-ordered cuprate, *Science* **331**, 189 (2011).
- [8] M. Mitrano, A. Cantaluppi, D. Nicoletti, S. Kaiser, A. Perucchi, S. Lupi, P. Di Pietro, D. Pontiroli, M. Riccò, S. R. Clark, D. Jaksch, and A. Cavalleri, Possible light-induced superconductivity in K_3C_{60} at high temperature, *Nature* **530**, 461 (2016).
- [9] F. Schlawin, A. Cavalleri, and D. Jaksch, Cavity-mediated electron-photon superconductivity, *Phys. Rev. Lett.* **122**, 133602 (2019).
- [10] O. Hart, G. Goldstein, C. Chamon, and C. Castelnovo, Steady-state superconductivity in electronic materials with repulsive interactions, *Phys. Rev. B* **100**, 060508(R) (2019).
- [11] M. Claassen, D. M. Kennes, M. Zingl, M. A. Sentef, and A. Rubio, Universal optical control of chiral superconductors and Majorana modes, *Nat. Phys.* **15**, 766 (2019).
- [12] P. W. Anderson, Plasmons, gauge invariance, and mass, *Phys. Rev.* **130**, 439 (1963).
- [13] C. M. Varma, Higgs boson in superconductors, *J. Low Temp. Phys.* **126**, 901 (2002).
- [14] D. Pekker and C. Varma, Amplitude/Higgs modes in condensed matter physics, *Ann. Rev. Condens. Matter Phys.* **6**, 269 (2015).
- [15] P. W. Anderson, Higgs, Anderson and all that, *Nat. Phys.* **11**, 93 (2015).
- [16] R. Sooryakumar and M. V. Klein, Raman scattering by superconducting-gap excitations and their coupling to charge-density waves, *Phys. Rev. Lett.* **45**, 660 (1980).
- [17] R. Sooryakumar and M. V. Klein, Raman scattering from superconducting gap excitations in the presence of a magnetic field, *Phys. Rev. B* **23**, 3213 (1981).
- [18] R. Grasset, T. Cea, Y. Gallais, M. Cazayous, A. Sacuto, L. Cario, L. Benfatto, and M.-A. Méasson, Higgs-mode radiance and charge-density-wave order in $2H-NbSe_2$, *Phys. Rev. B* **97**, 094502 (2018).
- [19] P. B. Littlewood and C. M. Varma, Gauge-invariant theory of the dynamical interaction of charge density waves and superconductivity, *Phys. Rev. Lett.* **47**, 811 (1981).
- [20] P. B. Littlewood and C. M. Varma, Amplitude collective modes in superconductors and their coupling to charge-density waves, *Phys. Rev. B* **26**, 4883 (1982).
- [21] R. Matsunaga, Y. I. Hamada, K. Makise, Y. Uzawa, H. Terai, Z. Wang, and R. Shimano, Higgs amplitude mode in the BCS superconductors $Nb_{1-x}Ti_xN$ induced by terahertz pulse excitation, *Phys. Rev. Lett.* **111**, 057002 (2013).
- [22] R. Matsunaga, N. Tsuji, H. Fujita, A. Sugioka, K. Makise, Y. Uzawa, H. Terai, Z. Wang, H. Aoki, and R. Shimano, Light-induced collective pseudospin precession resonating with Higgs mode in a superconductor, *Science* **345**, 1145 (2014).
- [23] A. F. Kemper, M. A. Sentef, B. Moritz, J. K. Freericks, and T. P. Devereaux, Direct observation of Higgs mode oscillations in the pump-probe photoemission spectra of electron-phonon mediated superconductors, *Phys. Rev. B* **92**, 224517 (2015).
- [24] N. Tsuji and H. Aoki, Theory of Anderson pseudospin resonance with Higgs mode in superconductors, *Phys. Rev. B* **92**, 064508 (2015).
- [25] H. P. O. Collado, J. Lorenzana, G. Usaj, and C. A. Balseiro, Population inversion and dynamical phase transitions in a driven superconductor, *Phys. Rev. B* **98**, 214519 (2018).
- [26] R. Shimano and N. Tsuji, Higgs mode in superconductors, *Ann. Rev. Condens. Matter Phys.* **11**, 103 (2020).
- [27] K. Katsumi, N. Tsuji, Y. I. Hamada, R. Matsunaga, J. Schneeloch, R. D. Zhong, G. D. Gu, H. Aoki, Y. Gallais, and R. Shimano, Higgs mode in the d -wave superconductor $Bi_2Sr_2CaCu_2O_{8+x}$ driven by an intense terahertz pulse, *Phys. Rev. Lett.* **120**, 117001 (2018).
- [28] M. A. Silaev, R. Ojajarvi, and T. T. Heikkilä, Spin currents driven by the Higgs mode in magnetic superconductors (2019), arXiv:1907.00539.
- [29] H. Krull, N. Bittner, G. S. Uhrig, D. Manske, and A. P. Schnyder, Coupling of Higgs and Leggett modes in non-equilibrium superconductors, *Nat. Comm.* **7**, 11921 (2016).
- [30] A. Moor, A. F. Volkov, and K. B. Efetov, Amplitude Higgs mode and admittance in superconductors with a moving condensate, *Phys. Rev. Lett.* **118**, 047001 (2017).
- [31] S. Nakamura, Y. Iida, Y. Murotani, R. Matsunaga, H. Terai, and R. Shimano, Infrared activation of the Higgs mode by supercurrent injection in superconducting NbN, *Phys. Rev. Lett.* **122**, 257001 (2019).
- [32] Z. M. Raines, A. A. Allocca, M. Hafezi, and V. M. Galitski, Cavity Higgs polaritons, *Phys. Rev. Research* **2**, 013143 (2020).
- [33] M. Puviani, L. Schwarz, X.-X. Zhang, S. Kaiser, and D. Manske, Current-assisted Raman activation of the Higgs mode in superconductors, *Phys. Rev. B* **101**, 220507 (2020).
- [34] V. L. Vadimov, I. M. Khaymovich, and A. S. Mel'nikov, Higgs modes in proximized superconducting systems, *Phys. Rev. B* **100**, 104515 (2019).
- [35] H. Uematsu, T. Mizushima, A. Tsuruta, S. Fujimoto, and J. A. Sauls, Chiral Higgs mode in nematic superconductors, *Phys. Rev. Lett.* **123**, 237001 (2019).
- [36] M. Buzzi, G. Jotzu, A. Cavalleri, J. I. Cirac, E. A. Demler, B. I. Halperin, M. D. Lukin, T. Shi, Y. Wang, and D. Podolsky, Higgs-mediated optical amplification in a non-equilibrium superconductor (2019), arXiv:1908.10879.
- [37] L. Schwarz, B. Fauseweh, N. Tsuji, N. Cheng, N. Bittner, H. Krull, M. Berciu, G. S. Uhrig, A. P. Schnyder, S. Kaiser, and D. Manske, Classification and characterization of nonequilibrium Higgs modes in unconventional superconductors, *Nat. Comm.* **11**, 287 (2020).
- [38] F. Yang and M. W. Wu, Theory of Higgs modes in d -wave superconductors (2020), arXiv:2001.06183.
- [39] W. Belzig, F. K. Wilhelm, C. Bruder, G. Schön, and A. D. Zaikin, Quasiclassical Green's function approach to mesoscopic superconductivity, *Superlattices Microstruct.* **25**, 1251 (1999).
- [40] N. Kopnin, *Theory of Nonequilibrium Superconductivity* (Oxford University Press, 2001).

- [41] See Supplemental Material for derivations and additional details.
- [42] Y. V. Nazarov, Novel circuit theory of Andreev reflection, *Superlattices Microstruct.* **25**, 1221 (1999).
- [43] J. Börlin, W. Belzig, and C. Bruder, Full counting statistics of a superconducting beam splitter, *Phys. Rev. Lett.* **88**, 197001 (2002).
- [44] F. S. Bergeret, P. Virtanen, A. Ozaeta, T. T. Heikkilä, and J. C. Cuevas, Supercurrent and Andreev bound state dynamics in superconducting quantum point contacts under microwave irradiation, *Phys. Rev. B* **84**, 054504 (2011).
- [45] B. Liu, H. Bromberger, A. Cartella, T. Gebert, M. Först, and A. Cavalleri, Generation of narrowband, high-intensity, carrier-envelope phase-stable pulses tunable between 4 and 18 THz, *Opt. Lett.* **42**, 129 (2017).
- [46] B. Liu, M. Först, M. Fechner, D. Nicoletti, J. Porras, T. Loew, B. Keimer, and A. Cavalleri, Pump frequency resonances for light-induced incipient superconductivity in $\text{YBa}_2\text{Cu}_3\text{O}_{6.5}$, *Phys. Rev. X* **10**, 011053 (2020).
- [47] G. Catelani, L. I. Glazman, and K. E. Nagaev, Effect of quasiparticles injection on the ac response of a superconductor, *Phys. Rev. B* **82**, 134502 (2010).
- [48] S. N. Artemenko and A. F. Volkov, Electric fields and collective oscillations in superconductors, *Soviet Physics Uspekhi* **22**, 295 (1979).

Supplemental Material

USADEL EQUATION AND OSCILLATING PART OF SUPERCONDUCTING ORDER PARAMETER

We consider a monochromatic electromagnetic irradiation with the time-dependent vector potential $\mathbf{A}(t) = \mathbf{A}_\Omega e^{-i\Omega t}$. The Higgs mode manifests itself in a time-dependent order parameter,

$$\langle \psi \rangle = \langle \psi_0 \rangle + \langle \psi_2 \rangle e^{-i2\Omega t}. \quad (17)$$

The quasiclassical Green's function $g_s(t, t')$ for a dirty superconductor with the diffusion constant D fulfills the time-dependent Usadel equation [39, 40],

$$i\{\tau_3 \partial_t, g_s\} + [\tau_3, g_s] - iD \nabla (g_s \circ \nabla g_s) = 0. \quad (18)$$

Here, the anti-commutator is defined as

$$\{\tau_3 \partial_t, g_s\} = \tau_3 \partial_t g_s(t, t') + \partial_{t'} g_s(t, t') \tau_3, \quad (19)$$

and $\nabla \cdot = \partial_{\mathbf{r}} \cdot - ie[\tau_3 \mathbf{A}(t), \cdot]$. The convolution operation between two objects f and g is defined as

$$(f \circ g)(t, t') = \int dt_1 f(t, t_1) g(t_1, t'). \quad (20)$$

The quasiclassical Green's function is written in Keldysh space and has the structure

$$g_s = \begin{pmatrix} \mathcal{G}_s^r & \mathcal{G}_s^k \\ & \mathcal{G}_s^a \end{pmatrix}. \quad (21)$$

The superconducting (SC) order parameter has the form $\langle \psi \rangle = i\tau_2 \cdot \langle \psi \rangle$. The matrices τ_α with $\alpha = 1, 2, 3$ are diagonal matrices with entries $\hat{\tau}_\alpha$, that is $\tau_\alpha = \text{diag}[\hat{\tau}_\alpha, \hat{\tau}_\alpha]$, where $\hat{\tau}_\alpha$ are the Pauli matrices in the Nambu space. The quasiclassical Green's function obeys the normalization condition $g_s \circ g_s = 1$. We will assume all quantities to be uniform within the SC or normal side of the junction. To leading order, the Green's function and order parameter can be expressed as

$$g_s(t, t') = g_0(t - t') + g_2(t, t'), \quad (22)$$

where the Fourier transforms of g_0 and g_2 are defined as

$$g_0(t - t') = \int \frac{d\epsilon}{2\pi} e^{-i\epsilon(t-t')} g_0(\epsilon),$$

$$g_2(t, t') = \int \frac{d\epsilon}{2\pi} e^{-i\epsilon_+ t + i\epsilon_- t'} g_2(\epsilon_+, \epsilon_-), \quad (23)$$

with $\epsilon_\pm = \epsilon \pm \Omega$. Due to the normalization condition for the stationary Green's function, $g_0 \circ g_0 = 1$, we obtain $g_2 \circ g_0 + g_0 \circ g_2 = 0$ which becomes $g_2(\epsilon_+, \epsilon_-) g_0(\epsilon_-) + g_0(\epsilon_+) g_2(\epsilon_+, \epsilon_-) = 0$ in the energy domain.

For the stationary quasiclassical Green's functions, we have [40]

$$\mathcal{G}_0^{r(a)}(\epsilon) = g_0^{r(a)}(\epsilon) \hat{\tau}_3 + i \hat{\tau}_2 f_0^{r(a)}(\epsilon), \quad (24)$$

$$\mathcal{G}_0^k(\epsilon) = [\mathcal{G}_0^r(\epsilon) - \mathcal{G}_0^a(\epsilon)] \tanh(\beta\epsilon/2), \quad (25)$$

where $\beta = 1/(k_B T)$, and

$$g_0^{r(a)} = f_0^{r(a)} \epsilon / \Omega = \epsilon / s_0^{r(a)}, \quad (26)$$

with $s_0^{r(a)} = i\sqrt{\frac{\Omega^2}{2} - (\epsilon \pm i\gamma)^2}$. Here, γ is the phenomenological Dynes broadening parameter. Inserting Eqs. (17) and (22) into Usadel equation (18) leads to

$$h_+ g_2(\epsilon_+, \epsilon_-) - g_2(\epsilon_+, \epsilon_-) h_- + 2g_0(\epsilon_-) - g_0(\epsilon_+) + iW_A [g_0(\epsilon) g_0(\epsilon_-) - g_0(\epsilon_+) g_0(\epsilon)] = 0, \quad (27)$$

with $h_\pm = \epsilon_\pm \tau_3 + \Omega i \tau_2$, $W_A = De^2 |\mathbf{A}_\Omega|^2$, and $g_0 = \tau_3 g_0 \tau_3$. By solving Eq. (27), we obtain the retarded and advanced components of the nonstationary term [28],

$$\mathcal{G}_2^{r(a)}(\epsilon_+, \epsilon_-) = \mathcal{G}_V^{r(a)}(\epsilon_+, \epsilon_-) + \mathcal{G}_H^{r(a)}(\epsilon_+, \epsilon_-), \quad (28)$$

with

$$\mathcal{G}_V^{r(a)}(\epsilon_+, \epsilon_-) = iW_A \left[\frac{\hat{\mathcal{G}}_0(\epsilon) - \hat{\mathcal{G}}_0(\epsilon_+) \hat{\mathcal{G}}_0(\epsilon) \hat{\mathcal{G}}_0(\epsilon_-)}{s_+ + s_-} \right]^{r(a)}, \quad (29)$$

and

$$\mathcal{G}_H^{r(a)}(\epsilon_+, \epsilon_-) = i \left[\frac{\hat{\mathcal{A}}_2 - \hat{\mathcal{G}}_0(\epsilon_+) \hat{\mathcal{A}}_2 \hat{\mathcal{G}}_0(\epsilon_-)}{s_+ + s_-} \right]^{r(a)}. \quad (30)$$

Here,

$$s_+^{r(a)} = i\sqrt{\frac{\Omega^2}{2} - (\epsilon_+ \pm i\gamma)^2}, \quad s_-^{r(a)} = i\sqrt{\frac{\Omega^2}{2} - (\epsilon_- \pm i\gamma)^2},$$

and $\mathcal{G}_V^{r(a)}$ and $\mathcal{G}_H^{r(a)}$ are due to the second order coupling to the vector potential and the Higgs mode, respectively.

The Keldysh component of $\mathcal{G}_2^k(\epsilon_+, \epsilon_-)$ can be expressed as the sum of a regular part $\mathcal{G}_2^{\text{reg}}$ and an anomalous part $\mathcal{G}_2^{\text{an}}$ [30, 48],

$$\mathcal{G}_2^k(\epsilon_+, \epsilon_-) = \mathcal{G}_2^{\text{reg}}(\epsilon_+, \epsilon_-) + \mathcal{G}_2^{\text{an}}(\epsilon_+, \epsilon_-), \quad (31)$$

with

$$\mathcal{G}_2^{\text{reg}} = \mathcal{G}_2^r(\epsilon_+, \epsilon_-) \tanh(\beta\epsilon_-/2) - \tanh(\beta\epsilon_+/2) \mathcal{G}_2^a(\epsilon_+, \epsilon_-), \quad (32)$$

and

$$\mathcal{G}_2^{\text{an}}(\epsilon_+, \epsilon_-) = \mathcal{G}_V^{\text{an}}(\epsilon_+, \epsilon_-) + \mathcal{G}_H^{\text{an}}(\epsilon_+, \epsilon_-). \quad (33)$$

The term $\mathcal{G}_V^{\text{an}}$ is expressed as

$$\mathcal{G}_V^{\text{an}} = iW_A \frac{[\tanh(\beta\epsilon_+/2) - \tanh(\beta\epsilon/2)][\hat{\mathcal{G}}_0^a - \hat{\mathcal{G}}_+^r \hat{\mathcal{G}}_0^a]}{s_+^r + s_-^a} + iW_A \frac{[\tanh(\beta\epsilon/2) - \tanh(\beta\epsilon_-/2)][\hat{\mathcal{G}}_0^r - \hat{\mathcal{G}}_+^r \hat{\mathcal{G}}_0^a]}{s_+^r + s_-^a}, \quad (34)$$

with the short notations $\hat{\mathcal{G}}_0^{r(a)} = \hat{\mathcal{G}}_0^{r(a)}(\epsilon)$ and $\hat{\mathcal{G}}_\pm^{r(a)} = \hat{\mathcal{G}}_0^{r(a)}(\epsilon_\pm)$. The term $\mathcal{G}_H^{\text{an}}$ is given by

$$\mathcal{G}_H^{\text{an}} = [\tanh(\beta\epsilon_+/2) - \tanh(\beta\epsilon_-/2)] \hat{\mathcal{A}}_2^{\text{an}}, \quad (35)$$

where $\mathcal{A}_H^{\text{an}}$ is obtained by replacing $\mathcal{G}_0^r(\epsilon_-)$ and s_-^r in the expression of $\mathcal{G}_H^r(\epsilon_+, \epsilon_-)$ with $\mathcal{G}_0^a(\epsilon_-)$ and s_-^a , respectively.

From the superconducting gap equation [40],

$$(\lambda) = -i\lambda \text{Tr}[\mathcal{A}_2 \mathcal{G}_s^k(t)], \quad (36)$$

where λ parametrizes the pairing interaction, we have

$$\int d\epsilon \text{Tr} [\mathcal{A}_2 \mathcal{G}_0^k(\epsilon)] = \int d\epsilon \text{Tr} [\mathcal{A}_2 \mathcal{G}_2^k(\epsilon_+, \epsilon_-)]. \quad (37)$$

Lengthy but straightforward calculations lead to

$$2 = iW_A \int d\epsilon \frac{B^r - B^a + B^{\text{an}}}{C^r - C^a + C^{\text{an}}}, \quad (38)$$

where

$$\begin{aligned} B^{r(a)} &= 2 \int d\epsilon b^{r(a)}(\epsilon) \tanh(\beta\epsilon_{\mp}/2), \\ B^{\text{an}} &= 2 \int d\epsilon b_+^{\text{an}}(\epsilon) [\tanh(\beta\epsilon_+/2) - \tanh(\beta\epsilon/2)] \\ &\quad + 2 \int d\epsilon b_-^{\text{an}}(\epsilon) [\tanh(\beta\epsilon/2) - \tanh(\beta\epsilon_-/2)], \\ C^{r(a)} &= \int d\epsilon [c^{r(a)}(\epsilon) \tanh(\beta\epsilon_{\mp}/2) - \tanh(\beta\epsilon/2)/s_0^{r(a)}], \\ C^{\text{an}} &= \int d\epsilon c^{\text{an}}(\epsilon) [\tanh(\beta\epsilon_+/2) - \tanh(\beta\epsilon_-/2)], \end{aligned}$$

with

$$\begin{aligned} b^{r(a)}(\epsilon) &= \left[\frac{\epsilon(\epsilon + \epsilon_+)s_- + \epsilon(\epsilon + \epsilon_-)s_+}{s_+s_0s_-(s_+ + s_-)^2} \right]^{r(a)}, \\ b_+^{\text{an}}(\epsilon) &= \frac{\epsilon(\epsilon + \epsilon_+)s_-^a + \epsilon(\epsilon + \epsilon_-)s_+^r}{s_+^r s_0^a s_-^a (s_+^r + s_-^a)^2}, \\ b_-^{\text{an}}(\epsilon) &= \frac{\epsilon(\epsilon + \epsilon_+)s_-^a + \epsilon(\epsilon + \epsilon_-)s_+^r}{s_+^r s_0^a s_-^a (s_+^r + s_-^a)^2}, \end{aligned}$$

and

$$\begin{aligned} c^{r(a)}(\epsilon) &= \left[\frac{s_+s_- + \epsilon_+\epsilon_- + \frac{2}{0}}{s_+s_-(s_+ + s_-)} \right]^{r(a)}, \\ c^{\text{an}}(\epsilon) &= \frac{s_+^r s_-^a + \epsilon_+\epsilon_- + \frac{2}{0}}{s_+^r s_-^a (s_+^r + s_-^a)}. \end{aligned}$$

One can see that c^{an} is obtained from c^r by replacing s_-^r with s_-^a .

AC CHARGE CURRENT

The charge current $I(t)$ can be decomposed into a DC component I_0 and an AC component I_2 with frequency 2ω ,

$$I(t) = I_0 + I_2 e^{-i2\Omega t}. \quad (39)$$

Using circuit theory [42–44], the charge current can be expressed as

$$I(t) = \frac{2\pi}{4e} \text{Tr} [\mathcal{A}_3 \hat{\mathcal{A}}^k(t)], \quad (40)$$

with the matrix current

$$\hat{\mathcal{A}}^k(t) = \frac{G_t}{2} [g_n, g_s]^k(t, t), \quad (41)$$

where G_t is the tunneling conductance of the NS junction. This leads to the following expressions,

$$I_0 = \frac{1}{4e} \int d\epsilon \text{Tr} [\mathcal{A}_3 \hat{\mathcal{A}}_0^k(\epsilon)], \quad (42)$$

$$I_2 = \frac{1}{4e} \int d\epsilon \text{Tr} [\mathcal{A}_3 \hat{\mathcal{A}}_2^k(\epsilon_+, \epsilon_-)], \quad (43)$$

with

$$\begin{aligned} \hat{\mathcal{A}}_0^k(\epsilon) &= \frac{G_t}{2} [\mathcal{G}_n^r \mathcal{G}_0^k(\epsilon) + \mathcal{G}_n^k(\epsilon) \mathcal{G}_0^a - \mathcal{G}_0^r \mathcal{G}_n^k(\epsilon) - \mathcal{G}_0^k(\epsilon) \mathcal{G}_n^a], \\ \hat{\mathcal{A}}_2^k(\epsilon_+, \epsilon_-) &= \frac{G_t}{2} [\mathcal{G}_n^r \mathcal{G}_2^k(\epsilon_+, \epsilon_-) + \mathcal{G}_n^k(\epsilon_+) \mathcal{G}_2^a(\epsilon_+, \epsilon_-) \\ &\quad - \mathcal{G}_2^r(\epsilon_+, \epsilon_-) \mathcal{G}_n^k(\epsilon_-) - \mathcal{G}_2^k(\epsilon_+, \epsilon_-) \mathcal{G}_n^a]. \end{aligned} \quad (44)$$

Since $\text{Tr}[\mathcal{G}_2^k(\epsilon_+, \epsilon_-)] = 0$, the AC charge current can be expressed as

$$I_2 = \frac{G_t}{8e} \int d\epsilon \text{Tr}(\mathcal{A}_3 \hat{\mathcal{X}}), \quad (45)$$

with

$$\hat{\mathcal{X}} = \mathcal{G}_n^k(\epsilon_+) \mathcal{G}_2^a(\epsilon_+, \epsilon_-) - \mathcal{G}_2^r(\epsilon_+, \epsilon_-) \mathcal{G}_n^k(\epsilon_-). \quad (46)$$

From this expression, one can verify that the AC charge current vanishes in the absence of the voltage bias, $I_2|_{eV=0} = 0$. In Fig. 3, we show the contributions from $\mathcal{G}_V^{r(a)}$ and $\mathcal{G}_H^{r(a)}$ in I_2 using Eqs. (45) and (46). The contributions to I_2 from g_V (denoted as $I_2^{\Delta_2=0}$) and g_H (denoted as I_H) are calculated by replacing g_2 in Eq. (46) with g_V and g_H , respectively. At resonance, i.e., $\omega = 0$, the contribution from $\mathcal{G}_V^{r(a)}$ is much smaller than that from $\mathcal{G}_H^{r(a)}$. This is due to the fact that $|\mathcal{G}_2^k|$ achieves its maximum and is much larger than W_A . For $\omega = 1$, the contribution from $\mathcal{G}_V^{r(a)}$ cannot be ignored and can be even slightly larger than that from $\mathcal{G}_H^{r(a)}$ at a small voltage bias.

We now try to get a compact expression for the AC charge current near resonance with $\omega \approx 0$ where the contribution from $\mathcal{G}_V^{r(a)}(\epsilon_+, \epsilon_-)$ in Eq. (28) can be ignored. Using

$$\mathcal{G}_0^r(\epsilon_+) \mathcal{A}_2 \mathcal{G}_0^r(\epsilon_-) = 2i \int d\epsilon \frac{\mathcal{A}_3}{s_+^r s_-^r} + u \mathcal{A}_2, \quad (47)$$

where the second term $u \mathcal{A}_2$ is unimportant in our derivation, Eq. (45) can be expressed as

$$\begin{aligned} I_2 &= \frac{G_t}{2e} \int d\epsilon \epsilon \left[\frac{\tanh(\frac{\epsilon_+ - eV}{2k_B T}) - \tanh(\frac{\epsilon_+ + eV}{2k_B T})}{s_+^a s_-^a (s_+^a + s_-^a)} \right. \\ &\quad \left. - \frac{\tanh(\frac{\epsilon_- - eV}{2k_B T}) - \tanh(\frac{\epsilon_- + eV}{2k_B T})}{s_+^r s_-^r (s_+^r + s_-^r)} \right]. \end{aligned} \quad (48)$$

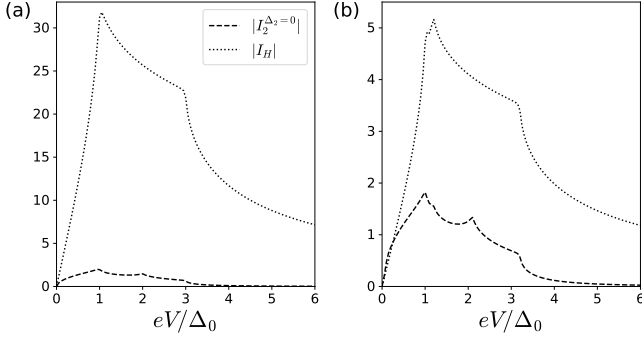


FIG. 3. The contributions from $\hat{g}_V^{r(a)}$ ($I_2^{\Delta_2=0}$, dashed lines) and $\hat{g}_H^{r(a)}$ (I_H , dotted lines) in calculating I_2 using Eqs. (45) and (46) for (a) $\Omega = \Delta_0$ and (b) $\Omega = 1.1\Delta_0$. The currents are given in units of $G_t W_A/e$.

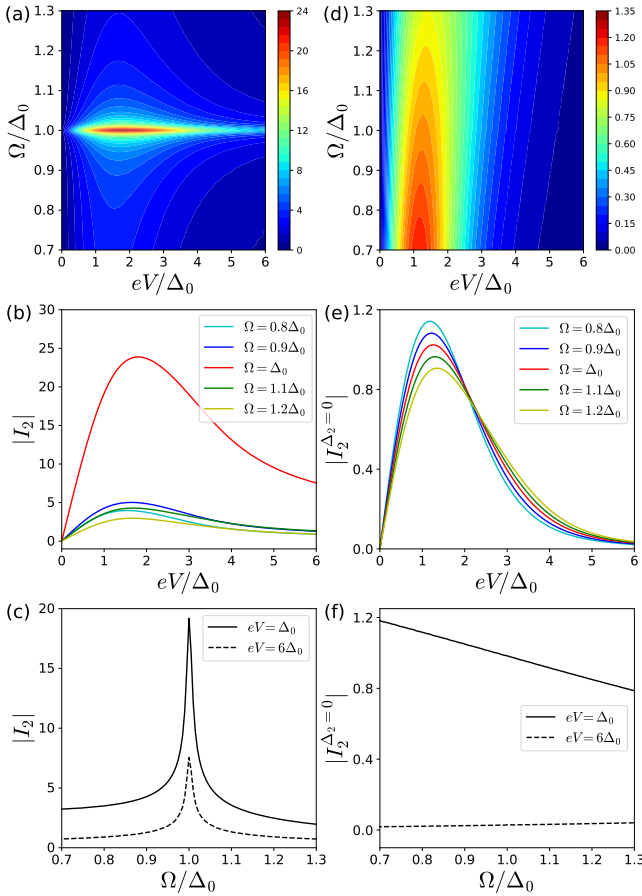


FIG. 4. (a) AC charge current $|I_2|$ plotted against voltage bias eV and irradiation frequency Ω . Panels (b) and (c) are line cuts of (a) at different Ω and eV , respectively. (d) AC charge current $|I_2^{\Delta_2=0}|$ in the absence of the Higgs mode, i.e., by artificially setting $\Delta_2 = 0$. Panels (e) and (f) are line cuts of (d) at different Ω and eV , respectively. The parameters are $T = 0.7T_c$, $\gamma = 0.01\Delta_0|_{T=0}$, and $W_A = 0.01\Delta_0|_{T=0}$.

Using the fact that $[s_+^{r(a)}]^2 - [s_-^{r(a)}]^2 = 4(\epsilon \pm i\gamma)$, this expression can be further simplified as,

$$I_2 = \frac{G_t}{8e} \int d\epsilon p(\epsilon) \left[\tanh\left(\frac{\epsilon - eV}{2k_B T}\right) - \tanh\left(\frac{\epsilon + eV}{2k_B T}\right) \right], \quad (49)$$

with

$$p(\epsilon) = \frac{1}{s_{++}^r} + \frac{1}{s_{--}^a} - \frac{1}{s_0^a} - \frac{1}{s_0^r}, \quad (50)$$

where

$$s_{++}^r = i\sqrt{\frac{2}{0} - (\epsilon + 2 + i\gamma)^2},$$

$$s_{--}^a = i\sqrt{\frac{2}{0} - (\epsilon - 2 - i\gamma)^2}.$$

Since $p(\epsilon) = p(-\epsilon)$, the expression for I_2 can be reduced to

$$I_2 = \frac{G_t}{4e} \int d\epsilon p(\epsilon) \tanh(\beta(\epsilon - eV)/2), \quad (51)$$

which can also be written as

$$I_2 = \frac{G_t}{4e} \int d\epsilon q(\epsilon) \left[\tanh\left(\frac{\epsilon_- - eV}{2k_B T}\right) - \tanh\left(\frac{\epsilon_+ - eV}{2k_B T}\right) \right], \quad (52)$$

with

$$q(\epsilon) = \frac{1}{s_+^r} - \frac{1}{s_-^a}. \quad (53)$$

Since $q(\epsilon) \approx 2/\epsilon$ for $\epsilon \gg 0$, we have $I_2 \propto 2/(eV)$ at large bias with $eV \gg 0$. In other words, at resonance and for large voltage bias, the AC current is inversely proportional to the voltage bias.

Similarly to Fig. (2) in the main text, we show the AC charge current behavior at a large temperature with $T = 0.7T_c$ in Fig. 4. A resonant behavior can be still observed at $\Omega = 0$. Fig. 4(b) also shows that $|I_2|$ exhibits a non-monotonic behavior with increasing bias and vanishes inversely proportional to the bias. Due to thermal excitations, the maximum of $|I_2|$ is shifted to larger voltages with $eV > 0$ compared to Fig. (2) in the main text. Kinks and local maxima are smeared by the thermal excitation as well.